(REGULATOR INFORMATION DISTRIBUTION STEEM (RIDS

ACCESSION NBR:8409050442 DOC.DATE: 84/08/22 NOTARIZED: NO DOCKET # FACIL:50-315 Donald C. Cook Nuclear Power Plant, Unit 1, Indiana 8 05000315

AUTHOR AFFILIATION

Exxon Nuclear Co., Inc. (subs. of Exxon Corp.)

RECIP.NAME

CHANDLER, J.C.

RECIPIENT AFFILIATION

DENTON, H.R. Office of Nuclear Reactor Regulation, Directors

SUBJECT: Forwards nonproprietary XN-NF-84-25(NP), "Mechanical Design.

Rept Suppl for DC Cook Unit 1 Extended Burnup Fuel

DISTRIBUTION CODE: TOOSD COPIES RECEIVED: LTR TENCL 14 SIZE: 1+94
TITLE: Non-Proprietary Version of Proprietary Topical Report

NOTES:

OL:10/25/74

05000315

	RECIPIENT ID CODE/NA	ME	COPIES		RECIPIENT ID CODE/NAM	E	COPI LTTR	
INTERNAL:	ADM/LFMB		1	0	ASLBP	11.	1	1
	-EL-D-/HDS3		1	0	NRR MORAN, D.	01	1	1
	REG FILE	02	2	2	RES		٠3	3
	RGN1		1	0	RGN2		1 -	0
	RGN3		1	0	RGN'4		1	.0
	RGN5		1	0				·
EXTERNAL:	ACRS.		1'5	. 0	NRC PDR	02	1	1.
	NSIC	05	1	: 1	NTIS	06	1	1٠

Production of the second of th

ngang gang ang panggang pangg Manggang panggang pa Anggang panggang pan

EXON NUCLEAR COMPANY, Inc.

2101 Horn Rapids Road

P. O. Box 130, Richland, Washington 93352

Phone: (509) 375-8100 Telex: 15-2878

August 22, 1984 JCC:116:84

Donald C. Cook Nuclear Plant Unit No. 1 Docket No. 50-315 License No. DPR-58 MECHANICAL DESIGN ANALYSES SUPPORTING HIGH BURNUP OPERATION OF NUCLEAR FUEL FABRICATED BY EXXON NUCLEAR COMPANY

Mr. Harold R. Denton, Director Office of Nuclear Reactor Regulation U.S. Nuclear Regulatory Commission Washington, D.C. 20555

Ref.: Letter, J.C. Chandler (ENC) to H.R. Denton (NRC), "Mechanical Design and LOCA ECCS Analyses Supporting High Burnup Operation of Fuel Fabricated by Exxon Nuclear," dated August 21, 1984 (JCC:113:84).

Dear Mr. Denton:

Enclosed for your use are fifteen copies of the following technical report issued by Exxon Nuclear Company:

XN-NF-84-25(NP), "Mechanical Design Report Supplement for D.C. Cook Unit 1; Extended Burnup Fuel Assemblies," dated April 1984.

At the request of American Electric Power Service Company (AEPSC), this documents is being transmitted directly by Exxon Nuclear. This report has been reviewed by AEPSC and will be referenced in subsequent docket action.

The enclosed report is the non-proprietary verion of Exxon Nuclear topical report XN-NF-84-25(P), which was transmitted to you by the reference letter. If you have any questions regarding this submission, please contact Mr. James G. Feinstein of AEPSC at (614) 233-2040.

Sincerely,

J.C. Chandler, Lead Engineer Reload Fuel Licensing

JCC:naa

cc: Mr. D.L. Wigginton (NRC) Mr. M.P. Alexich (AEPSC)

B409050442_B40B22_

1008

ni •

XN-NF-84-25 (NP)

MECHANICAL DESIGN REPORT SUPPLEMENT FOR
D.C. COOK UNIT 1
EXTENDED BURNUP FUEL ASSEMBLIES

AUGUST 1984

RICHLAND, WA 99352

EXON NUCLEAR COMPANY, INC.

8409050442

G

EXON NUCLEAR COMPANY, Inc.

XN-NF-84-25(NP)
Issue Date: 8/21/84

MECHANICAL DESIGN REPORT SUPPLEMENT FOR D.C. COOK UNIT 1 EXTENDED BURNUP FUEL ASSEMBLIES

Prepared:	N. L. Garner Project Engineer	<u>3/15/</u> 84 Date
Approved:	G. J. Busselman, Manager Fuel Design	11/5/87 Date
Concur:	R. B. Stout, Manager Licensing & Safety Engineering	9 1-02 8 4 Date
b	H. E. Williamson, Manager Neutronics & Fuel Management	<i>4<u>/9/8</u>4</i> Date
	J. M. Morgan, Manager Proposals & Customer Services Engineering	<u>4/:/</u> ;4 Date
	G. A. Sofer Manager Fuel Engineering & Technical Services	/ <i>ロ パパミご</i> り Date

NUCLEAR REGULATORY COMMISSION DISCLAIMER

IMPORTANT NOTICE REGARDING CONTENTS AND USE OF THIS DOCUMENT PLEASE READ CAREFULLY

This technical report was derived through research and development programs sponsored by Exxon Nuclear Company, Inc. It is being submitted by Exxon Nuclear to the USNRC as part of a technical contribution to facilitate safety analyses by licensees of the USNRC which utilize Exxon Nuclear-fabricated reload fuel or other technical services provided by Exxon Nuclear for light water power reactors and it is true and correct to the best of Exxon Nuclear's knowledge, information, and belief. The information contained herein may be used by the USNRC in its review of this report, and by licensees or applicants before the USNRC which are customers of Exxon Nuclear in their demonstration of compliance with the USNRC's regulations.

Without derogating from the foregoing, neither Exxon Nuclear nor any person acting on its behalf:

- A. Makes any warranty, express or implied, with respect to the accuracy, completeness, or usefulness of the information contained in this document, or that the use of any information, apparatus, method, or process disclosed in this document will not infringe privately owned rights;
- B. Assumes any liabilities with respect to the use of, or for damages resulting from the use of, any information, apparatus, method, or process disclosed in this document.

TABLE OF CONTENTS

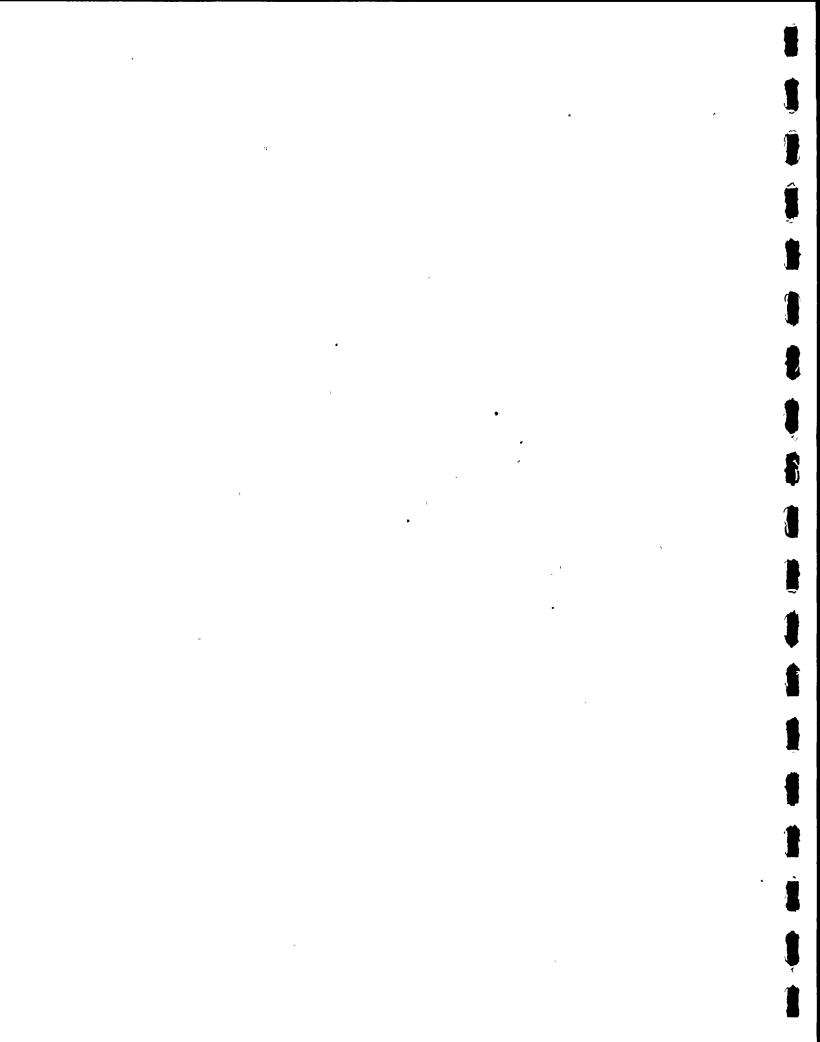
Sect	<u>ion</u>	Title	Page
1.0		INTRODUCTION	1
2.0		SUMMARY	1
3.0		DESIGN BASES	3
	3.1	CLADDING PHYSICAL AND MECHANICAL PROPERTIES	3
	3.2	CLADDING STRESS LIMITS	3
	3.3	CLADDING STRAIN LIMITS	5
	3.4	STRAIN FATIGUE	6
	3.5	FRETTING CORROSION AND WEAR	6
	3.6	CORROSION	7
	3.7	HYDROGEN ABSORPTION	7
	3.8	CREEP COLLAPSE	9
	3.9	FUEL ROD INTERNAL PRESSURE	10
	3.10	CREEP BOW	11
	3.11	OVERHEATING OF CLADDING	11
	3.12	OVERHEATING OF FUEL PELLETS	11
	3.13	FUEL ROD AND ASSEMBLY GROWTH	12
4.0		DESIGN DESCRIPTION	15
	4.1	FUEL ASSEMBLY	15
	12	FIIFL POD	15

TABLE OF CONTENTS (Continued)

Section	Title	Page
5.0	FUEL ASSEMBLY MATERIAL PROPERTIES	19
5.1	ZIRCALOY-4	19
5.2	FISSILE MATERIAL (URANIUM DIOXIDE)	28
5.3	INCONEL SPRINGS	32
6.0	MECHANICAL DESIGN EVALUATION	54
6.1	REACTOR OPERATING CONDITIONS FOR DESIGN	54
6.2	FUEL ROD EVALUATION	54
6.3	FUEL ASSEMBLY EVALUATION	70
7.0	REFERENCES	82
APPENDIX A -	DESIGN DRAWINGS	A-1

LIST OF TABLES

Table No.	<u>Title</u>	Page
3.1	STEADY STATE STRESS DESIGN LIMIT	13
4.1	FUEL ASSEMBLY DESIGN	17
5.1	CHEMICAL COMPOSITION ZIRCALOY-4	33
5.2	TABULATION OF CLADDING CORRELATIONS	34
5.3	URANIUM DIOXIDE IMPURITY LIMITS	35
5.4	CHEMICAL COMPOSITION OF INCONEL X-750 WIRE OR ROD	36
6.1	FUEL ROD PARAMETERS USED IN DESIGN EVALUATION	74
6.2	D.C. COOK UNIT 1 EXTENDED EXPOSURE STUDY - POWER AND FAST FLUX HISTORY FOR THE PIN WITH MAXIMUM DISCHARGE EXPOSURE	75
6.3	DUTY CYCLES	76



LIST OF FIGURES

Figure No.	<u>Title</u>	Page
3.1	STRESS THRESHOLD FOR IRRADIATED ZIRCALOY CLADDING TESTED IN AN IODINE ENVIRONMENT	14
5.1	DUCTILITY OF ENC ZIRCALOY-4 TUBING VERSUS TEMPERATURE	37
5.2	MECHANICAL STRENGTH OF ENC ZIRCALOY-4 TUBING VERSUS TEMPERATURE	38
5.3	REVIEW OF DATA PERTAINING TO THE EFFECT OF FAST NEUTRONS ON THE CHANGE IN YIELD STRESS IN ZIRCALOY	39
5.4	EFFECT OF FAST NEUTRON IRRADIATION AT 500°F (260°C) ON THE MECHANICAL PROPERTIES OF ZIRCALOY-2	40
5.5	COMPARISON OF CLADDING CREEPDOWN	41
5.6	AXIAL STRAIN VS. FAST NEUTRON FLUENCE FOR FUELED RODS	52
5.7	PWR ASSEMBLY GROWTH	43
5.8	CYCLIC FATIGUE DESIGN CURVE FOR IRRADIATED ZIRCALOY-2 OR -4 AT ROOM TEMPERATURE TO 600°F	44
5.9	GAP CLOSURE OF AS-FABRICATED GAP VERSUS IRRADIATION TIME	45
5.10	COMPARISON ON FISSION GAS RELEASE	46
5.11 [.]	MECHANICAL STRENGTH OF INCONEL X-750	47
5.12	POISSON'S RATIO OF INCONEL X-750	48
5.13	ELASTIC MODULUS OF INCONEL X-750	49
5.14	SHEAR MODULUS INCONEL X-750 VERSUS TEMPERATURE	50

LIST OF FIGURES (Continued)

Figure No.	<u>Title</u>	Page
5.15	THERMAL CONDUCTIVITY OF INCONEL X-750 VERSUS TEMPERATURE	51
5.16	MEAN THERMAL EXPANSION COEFFICIENT OF INCONEL X-750 FROM ROOM TEMPERATURE	52
5.17	INCONEL X-750 STRESS REDUCTION RATIO VERSUS FLUENCE	53
6.1	CONTACT STRESS FINITE ELEMENT MODEL	77
6.2	VIEW OF WELD JOINT REGION FINITE ELEMENT MODEL	78
6.3	D.C. COOK UNIT 1 STEADY STATE CLADDING STRAIN HISTORY	, 79
6.4	GAP SPACING DATA	80
6.5	ELONGATION STRAIN OF ENC FUEL AT D.C. COOK 1 E>1 MEV (X10E21 N/CM2)	81

D.C. COOK UNIT 1 EXTENDED BURNUP FUEL ASSEMBLIES

1.0 INTRODUCTION

This report provides the results of the mechanical design analyses for increasing the burnup level of Exxon Nuclear Company (ENC) Reload XN-5 and XN-6 fuel assemblies supplied for the D.C. Cook Unit 1 reactor, Cycles 6 and 7, respectively. The report supplements the base design report(1) by evaluating topics affected by the increased exposure conditions.

2.0 SUMMARY

The fuel design for the D.C. Cook Unit 1 reactor has been reanalyzed to support an increase in reactor cycle length. This increase from annual to 18-month cycles requires increases in the design analysis burnup level.

Mechanical design analyses were performed to evaluate cladding steady-state strain, transient stress and strain, fatigue, internal pressure, creep collapse, corrosion, hydrogen absorption, and fuel rod/fuel assembly irradiation growth. These analyses were performed to a peak assembly burnup of 41,000 MWd/MTU, a peak rod burnup of 43,700 MWd/MTU, and a peak pellet burnup of 48,000 MWd/MTU. Design criteria, consistent with current ENC practice, and the RODEX2 fuel performance code version approved by the USNRC in 1983, were used in the analyses. The results indicate that all the mechanical design criteria are satisfied.

o The maximum end-of-life (EOL) steady-state cladding strain was determined to be negative, thus meeting the 1.0% design limit.

- o The cladding stress and strain during power ramps, calculated under different overpower conditions, do not exceed the design stress corrosion cracking threshold or the 1.0% strain limit.
- o The cladding fatigue usage factor of 0.20 is within the 0.67 design limit.
- o The end-of-life fuel rod internal pressure is less than the system pressure.
- o The cladding diameter reduction due to uniform creepdown plus creep ovality after fuel densification is less than the minimum initial pellet/clad gap. This criterion prevents the formation of fuel column gaps.
- The maximum calculated EOL thickness of the oxide corrosion layer is less than 0.0007 inch, and the maximum calculated concentration of hydrogen in the cladding is 80 ppm. These values are within the design limits.
- o An evaluation of the fuel assembly growth and the fuel rod growth indicates that the fuel assembly design provides adequate clearances at the design burnup.

3.0 DESIGN BASES

The design considers effects and changes in physical properties of fuel assembly components which result from burnup.

The integrity of the fuel rods is ensured by analyzing the fuel to show that excessive fuel temperatures, excessive internal rod gas pressures, and excessive cladding stresses and strains do not occur. This end is achieved by showing the fuel rods to satisfy the design bases for normal operation and anticipated operational occurrences over the fuel lifetime. For each design basis, the performance of the most limiting fuel rod shall not exceed the specified limits.

The functional capability of the fuel assembly is ensured by analyzing the fuel assembly to show that the fuel system dimensions and properties remain within operational tolerances. This is achieved by showing that the fuel assemblies satisfy the design bases for normal operation and anticipated operational occurrences over the fuel lifetime.

3.1 CLADDING PHYSICAL AND MECHANICAL PROPERTIES

Zircaloy-4 combines a low neutron absorption cross section, high corrosion resistance, and high strength and ductility at operating temperatures. Principal physical and mechanical properties including irradiation effects on Zircaloy-4 are provided in Section 5.

3.2 CLADDING STRESS LIMITS

The design basis for the fuel cladding stress limits is that the fuel system will not be damaged due to fuel cladding stresses exceeding material capability. Conservative limits, shown in Table 3.1, are derived from the ASME Boiler and Pressure Vessel Code, Section III, Article III-2000.(3)

The cladding may also be damaged by the combination of volatile fission products and high cladding tensile stresses which may lead to stress corrosion cracking. (4,5) Stress corrosion cracking of fuel rod cladding is considered the principal failure mechanism for PCI failures encountered during changes in reactor operating conditions.(6,7,8) Even though unanimous agreement has not been reached on which chemical species enhances failure, the iodine atmosphere is usually considered the primary attacking media in irradiated fuel. If the stress level is low enough in the cladding, then stress corrosion cracking does not occur. Tests have been done under EPRI support(9,10,11) to evaluate a stress threshold associated with stress corrosion cracking in an iodine atmosphere. Figure 3.1 shows typical data from this program, and that the time dependence of stress corrosion rupture involves two processes. At the higher stresses (represented by the steep slope portion of Figure 3.1), the time to failure is largely controlled by the crack propagation process. At lower stresses (represented by the shallow slope portion of Figure 3.1), time to failure is largely controlled by a time-dependent crack nucleation process. Thus, if stress levels remain low enough, a flaw or crack that would subsequently propagate will not be nucleated.

The concept used to avoid failures from the stress corrosion crack failure mechanism from power ramps is to keep the fuel rods from operating above the stress threshold associated with the nucleation of a propagating stress corrosion crack. The modelling of the stress corrosion crack propagation process and methods for predicting the stress levels in fuel rods operating under prototype exposure histories incorporate many assumptions.

The design procedure used to evaluate ENC fuel rods uses a stress threshold determined from benchmarking studies using the RODEX2(12) and RAMPEX(13) codes. The design criterion for the transient stress limit resulting from a power ramp is to keep the predicted stress levels below the stress thresholds obtained in the benchmarking studies of test ramp cases.

The benchmarking test results were obtained from the Studsvik Inter-Ramp, Over-Ramp and Super Ramp test series. (13) Conservatism in the design bases is obtained by using only 80% of the code benchmarked failure stress threshold, by using conservative input values for the fuel rod dimensions in the design analyses and by assuming worse case power histories and ramp powers for the analysis. The concept of keeping below a stress threshold determined by code benchmarking protects against the initiation of a propagating flaw and empirically adjusts the design criteria to the test results from the simulations of limiting prototypic power ramps.

3.3 CLADDING STRAIN LIMITS

Tests(14,15) on irradiated tubing indicate potential for failure at relatively low mean strains. These tests include tensile, burst and split ring tests, and the data indicate a ductility ranging between 1.2% and 5% at normal reactor operating temperatures. The failures are usually associated with unstable or localized regions of high deformation after some uniform deformation. To prevent cladding failure due to plastic instability and localization of strain, the total mean circumferential cladding strain for transient and steady-state conditions is limited to 1%.

3.4 STRAIN FATIGUE

The number of cumulative strain fatigue cycles is limited to two-thirds (2/3) the design strain fatigue life.

Cyclic PCI loading combined with other cyclic loading associated with relatively large changes in power can cause cumulative damage which may eventually lead to fatigue failure. Cyclic loading limits are established to prevent fuel failures due to this mechanism. The design life is based on correlations which give a safety factor of 2 on stress amplitude or a safety factor of 20 on the number of cycles whichever is more conservative.(16)

3.5 FRETTING CORROSION AND WEAR

The design basis for fretting corrosion and wear is that fuel rod failures due to fretting shall not occur. Since significant amounts of fretting wear can eventually lead to fuel rod failure, the grid spacer assemblies are designed to prevent such wear. The spring dimple system in the spacer grid is designed such that the minimum spring/dimple forces throughout the design life are greater than the maximum fuel rod flow vibration forces. Testing of a wide variety of ENC fuel designs shows fuel rod wear depths at spacer contact points has typically ranged from 0.1 to 0.5 mils, although wear of up to 1.5 mils in depth has been observed. Examination indicates that the wear is due primarily to fuel rod loading and unloading and not due to fuel rod motion during the test. There has been

little or no difference between observed wear for 500 hour, 1000 hour and 1500 hour tests. No active fretting corrosion has been observed despite spacer spring relaxation of up to 100% in several test assemblies. Examination of a large number of irradiated rods has substantiated the minimal wear observed after loop tests. Numerous reload batches of the 15x15 design have operated in three reactors with no adverse effects due to fretting corrosion or wear.

3.6 CORROSION

Cladding oxidation and corrosion product buildup are limited in order to prevent significant degradation of clad strength. A PWR clad external temperature limit of 675°F is chosen, as corrosion rates are very slow below this temperature and therefore overall corrosion is limited.

This decrease in clad thickness (<10%) does not increase clad stresses above allowable levels.

Corrosion product buildup and the resulting temperature increases are calculated directly in the RODEX2 code.

3.7 HYDROGEN ABSORPTION

The as-fabricated cladding hydrogen level and the fuel rod cladding hydrogen level during life are limited to prevent adverse effects on the mechanical behavior of the cladding due to hydriding.(17,18) Hydrogen can be absorbed on either the outside or the inside of the cladding. The absorption of hydrogen can result in premature cladding failure due to reduced ductility and the formation of hydride platelets.

XN-NF-84-25 (NP) Page 8

The effects of hydrogen on mechanical properties have been investigated at hydrogen concentrations to about 1000 ppm.

The

effect on strength and ductility depends on such factors as:

- o The tube texture which tends to promote or minimize radially orientated hydrides.
- o Stress and temperature cycling which may promote reorientation of hydrides into radial directions. Tensile hoop stress tends to orient hydrides radially.(20)
- O Distribution of hydrides (hydride case layers on the I.D. or O.D. surface tend to promote brittle failures).
- o Ratio of cladding wall thickness to average length of hydride platelet.
 - o The fineness and uniformity in dispersion of the second phase precipitate tend to improve corrosion resistance and decrease hydrogen absorption.

The calculation of hydrogen concentration due to pickup from the coolant is calculated in the RODEX2 code. Hydrogen absorption from

inside the clad is minimized by careful moisture control during fuel fabrication.

3.8 CREEP COLLAPSE

The design basis for creep collapse of the cladding is that significant axial gaps due to fuel densification shall not occur and therefore that fuel failure due to creep collapse shall not occur. Creep collapse of the cladding can increase nuclear peaking, inhibit heat transfer, and cause failure due to localized strain.

If significant gaps form in the pellet column due to fuel densification, the pressure differential between the inside and outside of the cladding can act to increase cladding ovality. Ovality increase by clad creep to the point of plastic instability would result in collapse of the cladding. During power changes such collapse could result in fuel failure.

Through proper design, the formation of axial gaps and the probability of creep collapse can be significantly reduced. Typical ENC pellets are stable dimensionally. Irradiation data for ENC fuel rods, in addition to resintering tests performed at 1700°C for 24 hours on fabricated pellets, show that densification is not likely to exceed 2% volume. For high burnup designs the lot average resinter density change is limited to 2.0% by specification and is typically less than 1.5%. This specification ensures stable pellets during irradiation and limits the potential size of fuel column gaps.

An Inconel X-750 plenum spring is included in the ENC fuel rod design and the rods are pressurized with helium to help prevent the formation of gaps in the pellet column. The plenum spring provides a compressive force on the fuel column throughout the densification phase of the fuel life and the internal pressure prevents rapid clad creepdown as well as providing a good heat transfer medium for the fuel. No gaps larger than approximately 0.060 inch have been observed during gamma scans of many irradiated fuel rods.(22)

In order to guard against the unlikely event that sufficient densification occurs to allow pellet column gaps of sufficient size for clad flattening to occur, an analysis is performed using the method described in Section 4.5.5 of Reference 22, as submitted to the USNRC. With this method, creep ovality is calculated with the COLAPX code and cladding uniform creepdown is calculated with the RODEX2(23) code utilizing conservative design conditions. The cladding ovality increase and creepdown are summed, and at a rod average burnup which is beyond the point of complete fuel densification, the total creepdown shall not exceed the initial minimum diametral fuel cladding gap. This assures the prevention of pellet hangup due to cladding creep, allowing the plenum spring to close axial gaps until densification is substantially complete.

3.9 FUEL ROD INTERNAL PRESSURE

The internal gas pressure of the fuel rods shall not exceed the external coolant pressure. Significant outward circumferential creep which may cause an increase in pellet-to-cladding gap must be prevented

since it would lead to higher fuel temperature and higher fission gas release. Fuel rod internal pressure is calculated throughout life with the RODEX2 code.

3.10 CREEP BOW

Differential expansion between the fuel rods and lateral thermal and flux gradients can lead to lateral creep bow of the rods in the span between spacer grids. The design basis for fuel rod bowing is that lateral displacement of the fuel rods shall not be of sufficient magnitude to impact thermal margins. ENC fuel has been designed to minimize creep bow. Extensive post-irradiation examinations have confirmed that such rod bow has not reduced spacing between adjacent rods by more than 50%. The potential effect on thermal margins is negligible.

3.11 OVERHEATING OF CLADDING

The design basis for fuel rod cladding overheating is that transition boiling shall be prevented. Prevention of potential fuel failure from overheating of the cladding is accomplished by minimizing the probability that boiling transition occurs on the peak fuel rods during normal operation and anticipated operational occurrences. Margin to boiling transition is evaluated using applicable DNB correlations(24), with ENC's XCOBRA-IIIC(26) based PWR thermal-hydraulic methodology.

3.12 OVERHEATING OF FUEL PELLETS

Prevention of fuel failure from overheating of the fuel pellets is accomplished by assuring that the peak linear heat generation rate (LHGR) during normal operation and anticipated operational occurrences does not result in fuel centerline melting. The melting point of the fuel is adjusted for burnup in the centerline temperature analysis.

3.13 FUEL ROD AND ASSEMBLY GROWTH

The design basis for fuel rod and assembly growth is that adequate clearance shall be provided to prevent any interference which might lead to buckling or damage. Cladding and guide tube growth measurements of ENC fuel are used in establishing the growth correlations used for calculations.

Table 3:1 STEADY STATE STRESS DESIGN LIMIT

Stress Intensity Limits** Stress Category* Ultimate Yield Tensile Strength Strength 2/3 1/3 General Primary Membrane 1/2 Primary Membrane Plus Primary Bending 1.0 1.0 2.0 Primary Plus Secondary

- * Characteristics of the stress categories are defined as follows:
- a) Primary stress is a stress developed by the imposed loading which is necessary to satisfy the laws of equilibrium between external and internal forces and moments. The basic characteristic of a primary stress is that it is not self-limiting. If a primary stress exceeds the yield strength of the material through the entire thickness, the prevention of failure is entirely dependent on the strain-hardening properties of the material.
- b) Secondary stress is a stress developed by the self-constraint of a structure. It must satisfy an imposed strain pattern rather than being in equilibrium with an external load. The basic characteristic of a secondary stress is that it is self-limiting. Local yielding and minor distortions can satisfy the discontinuity conditions of thermal expansions which cause the stress to occur.
- ** The stress intensity is defined as twice the maximum shear stress and is equal to the largest algebraic difference between any two of the three principal stresses.

XN-NF-84-25(NP) Page 14

Figure 3.1 Stress Threshold for Irradiated Zircaloy Cladding Tested in an iodine Environment

4.0 DESIGN DESCRIPTION

4.1 FUEL ASSEMBLY

The 15x15 fuel assembly array includes 20 guide tubes, 204 fuel rods and one instrumentation tube. The grid spacers are of standard ENC bi-metallic design, and the fuel assembly tie plates are stainless steel castings with Inconel holddown springs. Drawings of the fuel assembly and fuel rod are given in Appendix A. Fuel assembly characteristics are summarized in Table 4.1.

4.2 FUEL ROD

The fuel rods consist of cylindrical ${\rm UO}_2$ pellets in Zircaloy-4 tubular cladding.

The Zircaloy-4 fuel rod cladding is cold worked and lightly stress relieved. Zircaloy-4 plug type end caps are seal welded to each end. The upper end cap has external features to allow remote underwater fuel rod handling. The lower end cap has a truncated cone exterior to aid fuel rod reinsertion into the fuel assembly during inspection and/or reconstitution.

Each fuel rod contains a 144.0 inch column of enriched UO_2 fuel pellets.

The fuel rod upper plenum contains an Inconel X-750 compression spring to prevent fuel column separation during fabrication and shipping, and during in-core operation.

Fuel rods are pressurized with helium which provides a good heat transfer medium and assists in the prevention of clad creep collapse.

XN-NF-84-25 (NP) Page 16

The fuel rod upper plenum contains an Inconel X-750 compression spring to prevent fuel column separation during fabrication and shipping, and during in-core operation.

Fuel rods are pressurized with helium which provides a good heat transfer medium and assists in the prevention of clad creep collapse.

Table 4.1 FUEL ASSEMBLY DESIGN

```
FUEL PELLET
     Fuel Material
     Pellet Diameter, (in.)
     Dish Volume Per Pellet (Total %)
     Pellet Length, (in.)
     Pellet Surface (\mu in AA)
     Pellet Density, (% TD)
CLADDING
     Clad Material
     Clad ID, (in.)
     Clad OD, (in.)
     Clad Thickness, Nominal, (in.)
     Clad Inside Surface (\mu in AA)
FUEL ROD
     Diametral Gap, Cold Nominal, (in.)
     Active Length, (in.)
     Plenum Length (in.)
     Total Rod Length, (in.)
     Fill Gas Pressure
```

Table 4.1

FUEL ASSEMBLY DESIGN (continued)

SPACER

Material

Rod Pitch

Envelope (in.)

GUIDE TUBE

Material

OD/ID Above Dashpot (in.)

OD/ID Dashpot (in.)

TIE PLATES

Material

HOLDDOWN SPRINGS

Material

CAP SCREWS

Materials

FUEL ASSEMBLY

Array

Assembly Pitch

Length

No. Spacers

No. Fuel Rods

No. Guide Tubes

No. Instrumentation Tubes

5.0 FUEL ASSEMBLY MATERIAL PROPERTIES

The material properties used in the design evaluation are described in this section. The Zircaloy cladding properties and the UO₂ fuel properties utilized are as incorporated in the RODEX2 and RAMPEX fuel performance codes. Inconel properties used in plenum spring evaluations are also included.

5.1 ZIRCALOY-4

5.1.1 Chemical Properties

Zircaloy-4 is used in three forms: (1) Coldworked and stress relieved cladding; (2) Recrystallized annealed tubing; and (3) Recrystallized annealed strip. The chemical properties in Table 5.1, in general, apply to all three forms. Where special properties apply for a certain form, it is so noted in the appropriate section.

XN-NF-84-25 (NP) Page 20

5.1.2 Physical Properties

a) Thermal Conductivity

Thermal conductivity for Zircaloy-4 is based on the NRC approved relation(28) used in RODEX2(12,23):

where:

b) Thermal Expansion

Thermal expansion used for Zircaloy-4(12,23) is

where

c) Elastic Modulus and Poisson's Ratio

The temperature dependence of the modulus of elasticity, E, used in design calculations is based on Duncombe(29) and is:

Poisson's ratio used in design calculations are:

d) Yield Strength

The minimum tensile properties for

Zircaloy-4 cladding are:

The ductility of Zircaloy-4 is given in Figure 5.1.

The yield strength of the cladding is used in setting convergence criteria in the pseudo-steady state calculations in RODEX2.(12) The 0.2% offset yield strength is determined from test data on ENC tubing (see Figure 5.2) and modified for the fluence dependence (see Figures 5.3 and 5.4). The relation used for 70 to 80% coldworked, stress relieved cladding(12,30) is:

where

 $Y_p = 0.2$ percent offset yield strength (psi)

T = cladding temperature (F)

F = fluence (n/cm²)

e) Steady State Creep Rate

The current NRC approved zircaloy creep rate used in fuel rod design calculations for creep collapse and stored energy is based on a general relationship developed by Watkins and Wood(31) as follows:

where

e_e = strain rate in %/hr

F = fast neutron flux (>1 Mev)

T = temperature, (°F)

se = applied stress, (psi)

The creep down measurements made for the Interramp, Overramp and Superramp programs and post irradiation profilometry measurements made on ENC fuel claddings were used to fit the creep coefficients for cladding typical of the ENC coldworked stress-relieved cladding (23), as shown on Figure 5.5.

where

R = (circumferential/radial) contractile strain ratio from an uniaxial axially loaded test

P = (axial/radial) contractile strain ratio from an uniaxial
 circumferentially loaded test

are the anisotropic parameters used in the creep relations generalized stress relation,(12,23,32) $\ _{\mbox{\scriptsize Se}}$

$$s_e = \frac{PR(s_h - s_z)E^2 + R(s_r - s_h)^2 + P(s_z - s_r)^2}{PR + P}$$

where h, r, z and e subscripts are for hoop, radial, axial and effective.

Typical values of the anisotropic parameters obtained for production cladding are R=2.0 and P=3.0.

f) Primary Creep

During power ramp conditions, the thermal-mechanical state of the fuel rod is evaluated with the RAMPEX code. (13) The higher stress levels encountered during power ramps can induce primary creep. The creep relation used in the RAMPEX evaluation is determined as the sum of an irradiation induced component and a primary creep component. The equivalent creep rate, e_e , is given by

$$e_e = e_I + e_D$$

where the irradiation induced component is

$$e_{I} = \exp[L_1 + L_2 \log S_e + L_4 \log F - \ln X_3 - L_2 \ln X_2 - L_3/(T + 459.4)]$$

and where the primary thermal component is

$$\dot{e}_p = \frac{1}{2 e_p} \left\{ \sinh (a s_e) \times \exp [H_1 - \ln X_3 + H_X (T - H_2)/(T + 459.4)] \right\}^2$$

The symbols in the preceding relations are defined as

$$H_X = H_3$$
 for $T \leq H_2$

=
$$H_4$$
 for $T > H_2$

$$a = (10^{-3}/X_2)*[H_5-H_6 (1-exp (-D/H_7))]$$

$$X_2 = [0.25 + (R/P)/(R+1)]^{0.5}$$

= ratio of effective stress to the hoop stress in a thin pressurized tube

$$X_3 = (R/2P) \times [(P+2)/(R+1)]/X_2$$

= ratio of hoop strain to effective strain in a thin pressurized tube

T = temperature = [F]

 \dot{e}_p = effective strain rate = [1/hr]

F = fast flux E.GT.1Mev = $[n/cm^2 \times sec]$

 S_e = effective stress = [psi]

D = fluence E.GT.1Mev = $[10^{21} \text{ n/cm}^2]$

The preceding relation has been fitted to pressurized cladding creep data on unirradiated tubing. For high strain rates, this relation approximates measured 0.2% yield strength values for both unirradiated and irradiated tubings. The values of the adjustable coefficients that correlate with the measured reactor interim profilometry data from cladding of ENC's coldworked and stressed relieved condition are:

g) <u>Transient and Accident Conditions</u>

For accident conditions, the plastic strain based on Hardy's data(33) is calculated as follows:

XN-NF-84-25/(NP) Page 26

`where

e_R = rupture strain

DT = rupture temperature minus actual mean clad temperature, $^{\circ}F$ ($T \leq 200^{\circ}F$)

and

where T_R is the rupture temperature in $^{\circ}C$, S_h is the engineering hoop stress in kpsi, and H is the ratio of the heating rate in $^{\circ}C/s$ to $28^{\circ}C/s$ (H varies from 0 to 1) as recommended in NUREG-0630.(34) The rupture strains are heating rate dependent as shown in Table 5.2.

h) Irradiation Induced Growth

Irradiation enhanced deformation processes in zircaloy have been attributed(35-40) to both stress and stress independent deformation mechanisms. The stress independent mechanism is termed growth and is dependent on preferential diffusion of irradiation-induced defects due to the anisotropic crystalline structure of zircaloy.

The growth relation used to evaluate the growth of coldworked fuel cladding in the RODEX2 code is based on an empirical fit of data collected in irradiated fuel rods. (41) The resultant relation is:

where

D = fast neutron fluence > 1° Mev, (n/cm^2)

e_q = axial growth strain, (cm/cm)

Rod growth data from 750 ENC rods irradiated in the Oyster Creek, Big Rock Point, H. B. Robinson, R. E. Ginna and Palisades Reactors were statistically analyzed to determine this relation. The graphical comparison of this design relation to data assembled in comparable irradiation and design conditions with data error bars is shown in Figure 5.6.

Annealed zircaloy is used for the guide tubes to reduce assembly growth and the possibility of bundle bowing where lateral gradients in the fast flux exist. The correlation developed for MATPRO(42) is:

where

 e_q = axial growth strain = [in/in]

T = material temperature = [K]

 F_z = texture factor

CW = cold work = [%]

D = fast fluence .G.T.1 Mev. = (n/cm^2)

and for annealed guide tube material

are the recommended material parameters to be used. This relation has been compared with measured length changes on irradiated ENC PWR fuel bundles (see Figure 5.7).

i. Fatigue Under Load Cycling

Cyclic mechanical strains can cause cumulative damage and subsequent failure which may be predicted by fatigue analysis techniques. O'Donnel and Langer(16) have developed a zircaloy fatigue analysis design curve which is presented in Figure 5.8. This curve is based on fatigue test data with a margin of 2 on stress or 20 on number of cycles, whichever is the most conservative.

5.2 FISSILE MATERIAL (URANIUM DIOXIDE)

5.2.1 Chemical Composition

a) Uranium Content

The uranium content shall be a minimum of 87.7% by weight of the uranium dioxide on a dry weight basis.

b) Stoichiometry

The oxygen to uranium ratio of the sintered fuel pellets shall be within the limits of 1.99 and 2.02.

c) Impurity Content

The impurity content shall not exceed the individual element and total content limits specified in Table 5.3, on a uranium weight basis.

XN-NF-84-25 (NP) Page 29

The total equivalent boron content (EBC) shall not exceed 4.0 ppm on a uranium weight basis. The total EBC is the sum of the EBC values of individual elements.

5.2.2 Thermal Properties

a) Thermal Expansion

The expansion model for $U0_2$ is based on Conway and Fincel's (43) relationship, i.e.,

where:

T = Temperature *F

 α = coefficient of thermal expansion, (in/in)/F

The curve of Conway and Fincel provides a conservative design limitation over the entire ${\tt UO}_2$ temperature spectrum.

b) Thermal Conductivity

The thermal conductivity function for UO_2 is based on data by Lyons, et al(44), and expressed as follows in the RODEX2(7) and GAPEX(28) codes:

where

T = temperature, °F

K = thermal conductivity = (BTU/[Hr x in x F])

 V_f = void fraction

5.2.3 Mechanical Properties

a) Mechanistic Fuel Swelling Model

The irradiation environment and fissioning events cause the fuel material to alter its volume and, consequently, its dimensions.

The following mechanisms are considered in the model:

- o densification, the as-fabricated porosity is reduced or annihilated;
- o solid fission products which are responsible for the "matrix swelling"; a large part of this is due to volatile fission products, such as cesium which can be reduced when the volatile fission products migrate out of the grains;
- o gaseous fission products which migrate to grain boundaries and form intergranular bubbles;
- o swelling accommodation by as-fabricated porosity which reduces the net apparent swelling;
- o hot pressing or swelling suppression in case of external restraint which limits or suppresses the gaseous swelling;
 .
- o columnar grain growth which results in radial fuel migration;
- o pellet cracking of fuel relocation under thermal stress which results in substantial gap closure.

The details of the model are described in Appendix K of the RODEX2 report. (23)

b) Fission Gas Release

The evaluation of fission gas release is done by the RODEX2 code.(23) For design evaluations of end-of-life pressures, pellet-cladding interaction and general thermal mechanical conditions, a physically based two-stage release model is used. First stage fission gas release is to grain boundaries and then the second stage release is from the grain boundaries to the interconnected free gas volume. This release model is described in detail in Appendix E of the RODEX2 report⁽²³⁾ and its correlation with measured data is described in the benchmarking section of the RODEX2 report. Figure 5.10 is graphical representation of the comparative correlation between measured and predicted release.

c) Melting Point

The value used for the UO₂ melting point (unirradiated) is 2805°C (5081°F). Based on measurements by Christensen, et al., $^{(45)}$ the melting point is reduced linearly with irradiation at the rate of 12.2°C (22.0°F) per 1022 fiss/cm³ or 32°C (57.6°F) per 104 MWd/MTU.

 $T_{\rm m} = 2805 - 32 B$

where:

 $T_m = melting point in °C$

 $8 = burnup in 10^4 MWd/MTU$

5.3 INCONEL SPRINGS

5.3.1 Chemical Composition

Coil springs are fabricated from Inconel X-750 wire or rod with an alloy composition in accordance with Table 5.4 (AMS 56998).

5.3.2 Physical Properties of Inconel

Inconel X-750 springs are used in the fuel rod plenum to compress the fuel column. These springs are made from wire stock formed into helical coil compression springs. The design properties of this material are indicated in Figures 5.11 through 5.16.

The stress relaxation due to irradiation and temperature is shown for Inconel X-750 in Figure 5.17.

Table 5.1 CHEMICAL COMPOSITION ZIRCALOY-4

Element

Composition, wt% Grade R60804 (RA-2)

Tin

Iron

Chromium

0xygen

Iron + Chromium

Maximum Impurities, wt%

Aluminum

Boron (2)

Cadmium (2)

Carbon

Chlorine

Cobalt

Copper

Hafnium

Hydrogen

Magnesium

Manganese

Molybdenum

Nickel

Nitrogen

Silicon

Titanium

Tungsten

Uranium (total)

Oxygen limit shall be 1500 ppm.

⁽¹⁾ (2) Boron and Cadmium content require ingot certification only.

Table 5.2
TABULATION OF CLADDING CORRELATIONS

Rupture emperature (°C)	<10°C/s Burst Strain (%)	>25°C/s Burst Strain (%)
600		
625		
650		
675		
700		
725		
750		
775		
800		
825		
850		•
875		
900		
925		
950		
975		
1000		
1025		
1050		
1075		
1100		
1125		ę.
1150		
1175		

1200

Table 5.3

URANIUM DIOXIDE IMPURITY LIMITS

The impurity content of sintered fuel pellets shall not exceed the specified individual element and total content limits on a uranium weight basis.

<u>Impurity</u>

ppm

Aluminum

Calcium plus Magnesium

Carbon

Chromium

Cobalt

Fluorine

Fluorine plus Chlorine

Hydrogen (including moisture)

Iron

Nickel

Nitrogen (total)

Silicon

Total Impurity Limit

Table 5.4 CHEMICAL COMPOSITION OF INCONEL X-750 WIRE OR ROD

The composition shall conform to the following percentages by weight, determined by wet chemical methods in accordance with ASTM E354, by spectrographic methods in accordance with Federal Test Method Standard No. 151, Method 112, or by other approved analytical methods.

Minimum

Maximum

Carbon

Manganese

Silicon

Sulfur

Chromium

Nickel + Cobalţ

Columbium + Tantalum

Titanium

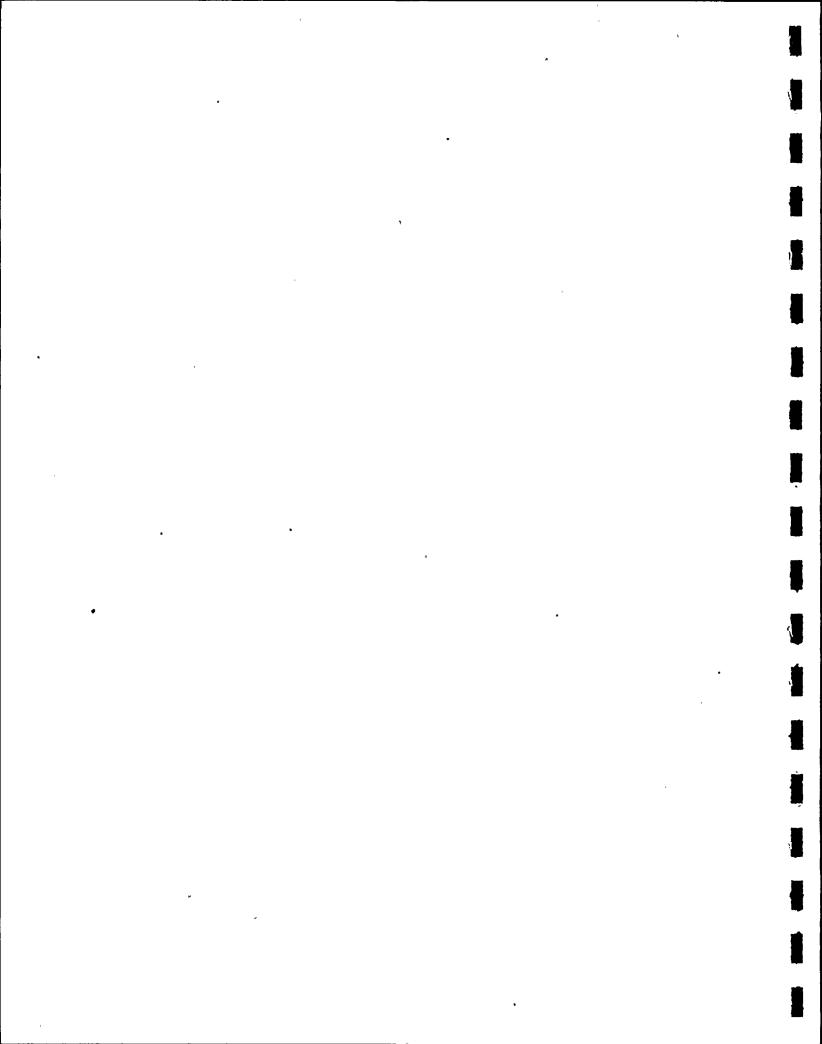
Aluminum

Iron

Cobalt

Copper

Figures 5.1 through 5.17 (pgs. 37-53) have been deleted.



6.0 MECHANICAL DESIGN EVALUATION

6.1 REACTOR OPERATING CONDITIONS FOR DESIGN

The high burnup fuel assembly design is based on the following reactor operating conditions:

Core power level (Nominal)	3250 MWt	
Coolant operating pressure (Nominal)	2250 psia	
Coolant flow rate (min. @ nominal power)		
Total	135.6 \times 10 ⁶ lb/hr.	
Active core	129.5×10^6 lb/hr.	
Heat generation fraction fuel rods	97.4%	
Coolant inlet temperature (Nominal)	536.3°F	
Number of assemblies in core	193	

The fuel shall be capable of load-follow operation between 50% and 100% of rated power, and not preclude the transients set forth in the FSAR. Reactor power ramping shall be in accordance with the limits established in the PREMACCX criteria, XN-NF-S30943, Rev. 2.(47)

6.2 FUEL ROD EVALUATION

6.2.1 Description

The fuel rods consist of cold worked and lightly stress relieved Zircaloy-4 cladding containing UO₂ pellets at 94.0% of theoretical density. The nominal diametral pellet cladding gap is 7.5 mils, the fuel column length is 144.0 inches, and total rod length is 152.065 inches. The upper plenum contains an Inconel X-750 spring. The rods are purged, pressurized with helium, and sealed with Zircaloy-4 end caps fusion welded to the cladding. Key fuel rod parameters used as input to the design analyses are listed in Table 6.1.

6.2.2 Design Criteria

- a) Cladding steady-state stresses shall not exceed the limits described in Article III-2000 of Reference 3, as defined in Table 3.1.
- b) Maximum cladding strain shall not exceed 1.0% at end-of-life (EOL), or 1.0% during power transients.
- c) During power transients, the maximum hoop stress in the cladding is limited to a value of ksi to avoid failure by stress corrosion cracking. This value of ksi corresponds to 80% of the failure threshold value, as determined by benchmarking(13) for the standard ENC cladding.
- d) The cumulative usage factor for cyclic stresses shall not exceed 0.67.
- e) The fuel rod internal pressure at the end of the design life shall not exceed the system operating pressure.
- f) The fuel rods shall be designed, considering initial prepressurization, clad thickness, and plenum spring characteristics, such that significant axial gaps cannot form during the fuel life so that clad creep collapse cannot occur. Analysis of the cladding ovality and creepdown shall show that,

 the overall creepdown is less than the BOL minimum specified cold pellet/cladding gap.
- g) Fuel rod creep bow throughout the design life of the assemblies shall be limited so as to maintain licensing and operational limit restraints.

- h) For the projected fuel rod design lifetime and operating conditions, the hydrogen content of the cladding shall not exceed 300 ppm, on a cladding weight basis, under the most adverse projected power conditions within coolant chemistry limits. Cladding wall thinning due to generalized corrosion shall not exceed over the projected fuel rod lifetime.
- i) The fuel rod plenum spring shall maintain a positive compression on the fuel column during shipping and during the fuel densification stage.
- j) Fuel rod growth shall be accommodated by axial clearance between the rod and the assembly tie plates.
 - k) Cladding Temperatures shall not exceed:

Inside Surface

Outside Surface

Volumetric Average

1) Pellet temperatures shall not exceed the melting temperature during normal operation and anticipated transients.

6.2.3 Fuel Rod Analysis

a) Cladding Steady-State Stresses

Each individual stress as described in the following paragraphs was calculated at both the inner and outer surfaces of the cladding.

Primary Stresses

Primary Membrane Stresses

The primary membrane stresses are produced by the coolant pressure and fuel rod fill gas pressure. The stresses are calculated by the Lame' equations recommended by P. Shariffi and E. P. Popov. (48)

$$s_{hoop} = [P_iR_i^2 - P_oR_o^2 + (R_iR_o/r)^2 (P_i-P_o)] / (R_o^2-R_i^2)$$

$$s_{radial} = [P_iR_i^2 - P_oR_o^2 - (R_iR_o/r)^2 (P_i-P_o)] / (R_o^2 - R_i^2)$$

$$s_{axial} = (s_{hoop} + s_{radial}) /2.0$$

where

s = primary membrane stress, psi

 P_0 = external pressure, psi

P_i = internal pressure, psi

r = any radius in the cladding, inches

R_i = internal radius, inches

 R_0 = outside radius, inches

Primary Bending Stresses

Bending stresses due to ovality are calculated with Timoshenko's equation (49).

shoop
$$\pm$$
 shoop $\left(1 \pm \frac{6U}{t}\right) \frac{P_a}{P_a-P}$

where:

shoop = Lame' primary membrane stress, psi

$$U = \underbrace{\frac{\text{ovality}}{4}} = \underbrace{\frac{\text{ID}_{\text{max}} - \text{ID}_{\text{min}}}{4}}$$

t = minimum 2 wall thickness

Pa = critical collapse pressure for perfect tube, psi

$$P_a = \frac{E}{4(1-\nu^2)} \frac{t}{r}^3$$

$$P = P_0 - P_1$$

E = Elastic Modulus,

 ν = Poisson's Ratio

r = mean radius, inch

Secondary Stresses

Cladding Thermal Gradient Stresses · ·

Fuel rods operate with a temperature gradient across the cladding wall which may result in significant thermal stresses. Assuming no stress relaxation, thermal stresses are calculated by (50):

$$s_{hoop} = \frac{E \alpha \Delta T}{2(1-\nu) \ln \frac{r_0}{r_i}} \left[1 - \frac{\left(\frac{r_0^2}{r^2} + 1\right)}{\left(\frac{r_0^2}{r_i^2} - 1\right)} \ln \frac{r_0}{r_i} - \ln \frac{r_0}{r} \right]$$

$$s_{\text{axial}} = \frac{E \alpha \Delta T}{2(1-\nu) \ln \frac{r_0}{r_i}} \left[1 - \frac{2}{\left(\frac{r_0^2}{r_i^2} - 1\right)} \right] \ln \frac{r_0}{r_i} - 2 \ln \frac{r_0}{r}$$

sradial = saxial - shoop

where

E = Elastic Modulus

= Coefficient of Thermal Expansion

AT = Temperature Gradient, from RODEX2 code

 ν = Poisson's Ratio

Restrained Thermal Bow

Stress due to circumferential gradients are conservatively estimated using relationships from Timoshenko and Gere (51).

$$s_{axial} = \frac{+}{2} \frac{E \alpha \Delta T}{2}$$

$$s_{hoop} = \frac{+}{2} \frac{E \alpha \Delta T}{2(1-\nu)}$$

where:

E = Elastic Modulus

 α = thermal expansion coefficient

ΔT = temperature differential around a tube assumed for design calculations to be equal to 20°F.

 ν = Poisson's Ratio

Restrained, Mechanical Bow

Stress from mechanical bow between spacers, assuming maximum-as-built fuel rod bow is zero, is taken from $Roark^{(52)}$:

$$s = \frac{8Era}{L^2}$$

where:

E = Elastic Modulus

r = outer radius, inch

L = distance between spacers, inches

a = maximum rod bow

Flow Induced Vibration Stresses

Vibrational stresses due to flow induced vibrations is calculated with the Paidoussis' (53,54) analysis which assumes the following:

- The structural stiffness of the fuel rod is due to the cladding only.
- 2) The sections of the fuel rod between spacers and/or tie plate supports are modelled structurally as a simple beam with pinned ends.
- 3) Flow velocity, viscosity, and virtual mass for the amplitude calculations are evaluated as suggested by Paidoussis.

$$s_{axial} = \frac{5\pi^2 \text{ Erd}}{2}$$

where:

d = vibration amplitude

Contact Stress From Spacer Springs

The contact stresses at the spring locations are calculated using the finite element model shown in Figure 6.1. Calculations were performed with the ANSYS(46) general purpose finite element code. The circumferential and axial stresses induced by the contact load are incorporated into the results.

Combined Stresses

The applicable stresses in each orthogonal direction were combined to get the maximum stress intensities. The analysis was performed at beginning-of-life (BOL) and end-of-life (EOL) at cold and hot

conditions. The maximum stress intensities given below did not exceed the stress limits.

Stress Intensity (psi)

Maximum

Limit

Primary Membrane

Primary Membrane + Bending

Primary + Secondary

Fuel Rod End Cap

Zircaloy end caps are seal welded to each end of the fuel rod cladding. The stress analysis is performed at the lower end cap since the maximum temperature gradients occur at this end.

The mechanical stress is caused by the pressure differential across the rod wall and by the axial load of the pellet stack weight and the plenum spring force. The thermal stress is caused by the temperature gradient between the end cap and the heat generating pellets. The stress analysis is for the standard ENC end cap design and envelopes both PWR and BWR applications.

The ANSYS code, (46) which allows thermal as well as stress analyses, was used to model the subject rod region. The problem was solved by a thermal pass and a stress pass, where the stress analysis used the results of the thermal analysis as part of its input. The model is in axisymmetric geometry and was set-up such that the element system could be used in both analyses. The weld-joint region of the model is shown in Figure 6.2. The maximum weld stress intensity of psi is well below the design limit of psi.

b) Steady State Strain Analyses

The cladding steady-state strain was evaluated with the RODEX2(23) code, latest version, as approved by the USNRC in 1983. The code calculates the thermal-hydraulic environment at the cladding surface, the pressure inside the cladding, and the thermal, mechanical and compositional state of the fuel and cladding. Calculations are performed for the worst expected fuel rod power and fast flux history to determine a conservative history in terms of cladding strain.

In addition to evaluation of the fuel rod steady-state cladding strain, RODEX2 determines the initial conditions for fuel rod power ramping analyses and the minimum fuel rod internal pressures for cladding creep analyses. Pellet density, swelling, densification, and fission gas release or absorption models, and cladding and pellet diameters are input to RODEX2 to provide the most conservative subsequent ramping or collapse calculations for the reference fuel rod design.

The fuel rod performance characteristics modelled by the RODEX2 code are:

- o Gas Release and Absorption
- o Radial Thermal Conduction and Gap Conductance
- o Free Rod Volume and Gas Pressure Calculations
- o Pellet-Cladding Interaction
- o Fuel Swelling, Densification, Cracking and Crack Healing
- o Cladding Creep Deformation and Irradiation Induced Growth

The calculations are performed on a time incremental basis with conditions updated at each calculated increment so that the power

history and path dependent processes can be modelled. The axial dependence of the spatial power and burn-up distributions are handled by dividing the fuel rod into a number of fuel segments which are modelled as radially dependent regions whose axial deformations and gas release are summed. Power disributions can be changed at any desired time and the coolant and cladding temperatures are readjusted at all axial nodes. Deformations of the fuel and cladding and gas release are incrementally calculated during each period of assumed constant power generation. Gap conductance is calculated for each of these incremental calculations based on gas release throughout the rod and the accumulated deformation at the center of each axial region within the fueled region of the rod. These deformation calculations consider fuel densification, swelling and cracking, thermal expansion, cladding creepdown, irradiation induced growth, and fuel creep and crack healing.

The peak discharge burnup fuel rod was analyzed for maximum EOL cladding strain. The design power history for this rod is summarized in Table 6.2. The result of the steady state strain analysis has been plotted in Figure 6.3. The vertical axis is the variation of cladding internal radius (DRCC = R - R [BOL]) in mils at the axial location of maximum strain. The horizontal axis is exposure time in hours. The analysis shows that the cladding is always under negative circumferential strain. Thus, the criterion of 1.0% maximum at EOL is satisfied. The minimum strain, strain at EOL, and the net outward creep strain for the axial region with the maximum positive strain increase are as follows:

Minimum Strain, % -0.67

Strain at EOL, % -0.38

Positive Increase, % 0.29

c) Ramp Stress and Strain Analysis

The clad response during ramping power changes is calculated with the RAMPEX code.(13) This code calculates the pellet-cladding interaction during a power ramp. The initial conditions are obtained from RODEX2 output. The RAMPEX code considers the thermal condition of the rod in its flow channel and the mechanical interactions that result from fuel creep, crack healing, and cladding creep at any desired axial section in the rod during the power ramp. As compared to RODEX2, RAMPEX additionally models the pellet cladding axial stess interaction, primary creep with strain hardening, the effects of pellet chips and localized stresses due to ridging. The benchmarking of the 1981 versions of these codes has determined a failure threshold stress for ENC cladding, 80% of which is used as a design limit.

The power history assumed for this analysis was the same as that used for steady-state strain analysis (Table 6.2). This power history was divided into three cycles, modelling the projected fuel shuffling during the fuel life. The conditions at the end of each cycle obtained with the RODEX2 code are used as input data for the RAMPEX code. End-of-cycle conditions are used in order to simulate chip relocation effects during fuel shuffling.

The rods under consideration were ramped to the maximum power in accordance with the PREMACCX criteria. (47) In addition, the maximum

clad strains due to each ramp were examined. The maximum strains, including primary and secondary thermal creep, were below the 1% strain limit.

d) Cladding Fatigue Usage

In addition to the ramp strain analyses, a fatigue usage factor for the cladding was calculated. The calculations were based upon the typical duty cycles summarized in Table 6.3. As in the cladding ramp strain analysis, the power ramp rate for reactor startup was assumed to follow ENC's PREMACCX preconditioning recommendation. Cladding stress amplitudes for the various power cycles were determined from RAMPEX analyses. The initial conditions were obtained from RODEX2 outputs.

RAMPEX analyses were run for each cycle at the plane of maximum contact pressure. Power swings from 0% to 100% power were run to the F_Q^T limit for the peak rod and a proportionate increase for other rods. Power swings from an intermediate power to 100% power were run to 112% of nominal power to account for potential reactor power distribution variations.

The allowed number of stress cycles is determined by conservative relations deduced from the fatigue curves of O'Donnel and Langer.(16) Results of the analysis are shown in Table 6.4. The overall fatigue usage factor of 0.20 is within the 0.67 design limit.

e) Internal Pressure

A RODEX2 analysis was performed to evaluate the end-of-life (EOL) fuel rod internal pressure. To prevent cladding instability, the rod internal pressure cannot exceed the system pressure or else the cladding may creep away from the pellet, which increases the fuel rod pellet temperatures. Higher fuel temperatures result in increased fission gas release

and, therefore, higher internal rod pressures. The results of this analysis show the EOL internal rod pressure does not exceed the system pressure of 2250 psia. The fuel rod will, therefore, remain stable throughout the expected power history.

f) Creep Collapse

Creep collapse calculations are performed with the RODEX2(23) and COLAPX(55,56) codes in accordance with the method described in the extended burnup report.(22) The RODEX2 code determines the cladding temperature and internal pressure history based on a model which accounts for changes in fuel rod volumes, fuel densification and swelling, and fill gas absorption. Minimum fill gas pressure, maximum fuel densification, minimum cladding wall thickness and nominal pellet dimensions are assumed. The reactor coolant, fuel rod temperature, and internal pressure histories generated by the RODEX2 analysis are input to the COLAPX code along with a conservative statistical estimate of initial cladding ovality and the fast flux history. The power and fast neutron flux histories for the peak power rod are utilized. The COLAPX code calculates, by large deflection theory, the ovality of the cladding as a functon of time while the uniform cladding creep down is obtained from the RODEX2 analysis.

If significant gaps (>1.3 rod diameter) are not allowed to form, then ovality, as predicted by the COLAPX evaluation, cannot occur beyond the point of fuel support. The ENC fuel rod design uses an Inconel X750 plenum spring to maintain an axial load on the pellet column well beyond the time when pellet densification is complete. This assists in the prevention of axial gaps. The limited pellet resinter densification also

assures the presence of stable fuel so that the formation of significant gaps is prevented, and so that clad support is available during the life of the fuel.

In order to guard against the highly unlikely event that enough densification occurs to form pellet column gaps of sufficient size to allow clad flattening, the following evaluation was performed. The combination of cladding ovality increase calculated with COLAPX

and the diametral creepdown calculated with RODEX2 was determined. At a rod average burnup of when densification is essentially complete, the combined creepdown the cladding minor axis does not exceed the minimum initial diametral fuel cladding gap

This allows the fuel column to relocate axially without the formation of axial gaps so that creep collapse will not occur.

g) Rod Bowing

Fuel rod bow is determined throughout the life of the fuel assembly so that reactor operating thermal limits can be established. These limits include the minimum critical heat flux ratio associated with protection against boiling transition and the maximum fuel rod LHGR associated with protection of metal-water reaction and peak cladding temperature limits for a postulated loss of coolant accident (LOCA).

ENC's rod bow measurements have been used to establish an empirical model for determining rod bow as a function of burnup which is used to calculate thermal limits.

The gap spacing data which is summarized in Figure 6.4 shows that the bow tends to stabilize at higher burnups. In addition, the fuel at high burnups is not limiting from a thermal margin standpoint due to its lower power.

h) Corrosion Layer and Hydrogen Absorption Analyses

The thickness of the corrosion layer and the amount of hydrogen absorbed by the cladding have been evaluated with the RODEX2 code for the peak discharge fuel rod power history. An initial maximum hydrogen content of 35 ppm was assumed, giving the following results:

Calculated Allowed

Hydrogen content (PPM)

Thickness of Corrosion Layer (in)

i) Fuel Rod Plenum Spring ·

The major functional requirements on the plenum spring occur during shipment and during the densification of the fuel. Since both of these situations occur relatively early in the life of the fuel, no reanalysis is required for extended burnup.

j) Fuel Rod Growth

Growth data from ENC PWR assemblies which have burnups to 40000 MWD/MTU are shown in Figure 5.6. Growth strain was correlated to fast fluence. The fuel rod growth model has been incorporated into the RODEX2 code. The calculated growth for the maximum rod burnup was

Conservatively assuming no guide tube growth, and adding a design tolerance on rod growth, a minimum end-of-life clearance margin of is available.

k) Cladding Temperature

A RODEX2 analysis was performed for the D.C. Cook
Unit 1 design fuel rod to evaluate the peak cladding temperatures during the

design life of the fuel. The results, using conservative inputs, are as follows:

Calculated Design Criteria

Clad I.D. (°F)
Clad O.D. (°F)
Volumetric Avg. (°F)

1) Fuel Pellet Temperature

Fuel pellet temperatures reach a peak early in life; therefore, no reanalysis is required for extended burnup.

6.3 FUEL ASSEMBLY EVALUATION

6.3.1 General Description

The fuel assemblies consist of a 15x15 array occupied by 204 fuel rods, 20 guide tubes and one instrument tube. Seven Zircaloy-4 spacers with Inconel 718 springs are positioned along the length of the assembly to locate the fuel rods and tubes, and are attached to the guide tubes by resistance spot weld. The guide tubes are mechanically attached to the upper and lower tie plates to form the structural skeleton of the fuel assembly.

6.3.2 Design Criteria

The mechanical design criteria for the fuel assembly are to provide for:

- o Dimensional Compatibility
- o Differential Thermal Expansion and Irradiation Growth Allowance
- o Fuel Rod Support
- o Fuel Assembly Holddown
- o Upper Tie Plate Removability
- o Handling and Storage Limits

Since the design is unchanged, only the irradiation growth allowance and the fuel rod restraint are affected by the extended burnups.

Specifically, the criteria require the design to provide adequate clearance between the tie plates to accommodate fuel rod growth, and adequate clearance between the fuel assembly and core plates to accommodate fuel assembly growth. The criteria for fuel rod support is to provide for sufficient spring force at EOL to minimize flow-induced vibrations and to prevent fretting corrosion at the spacer-fuel rod contact points, considering the effects of irradiation-induced spring force relaxation.

6.3.3 Design Analysis

Fuel Assembly Growth - The limiting condition for fuel assembly growth is at end-of-life after cooldown. Because of the higher coefficient of thermal expansion for the stainless steel core structure relative to the Zr-4 guide tubes, differential thermal expansion increases the assembly/internals structure clearance during heatup and reduces the clearance upon cooldown. The guide tube growth data for ENC irradiated fuel assemblies has generally been conservatively predicted by the MATPRO(42) data for annealled Zr-4. Projecting the D.C. Cook assembly growth measurements (Figure 6.3) to the enveloping 43,700 MWd/MTU peak rod burnup, provides a conservative margin of about 4% between the D.C. Cook assembly growth and that given by MATPRO. The maximum EOL fuel assembly length predicted by MATPRO assuming the peak rod average fluence for the guide tubes is inches, which leaves inch clearance with the core plate to core plate separation of 160.50 inches.

Spacer Spring Relaxation - The Inconel-718 spacer springs are known to relax during irradiation and the fuel rod cladding tends to creepdown. Together, these two characteristics combine to reduce the spacer spring force on a fuel rod during its lifetime. These characteristics have been considered in the design of the spring to assure an adequate holding force when the assembly has completed its design operating life.

spring holding force can be very low without resulting in fretting damage to the cladding. Extensive flow tests have been performed on ENC assemblies under various spacer spring load conditions. These tests have covered the range of no spring relaxation (i.e., new fuel) to total relaxation. In testing of up to 1000 hours duration, there was no measurable fretting wear, with up to 100% relaxation provided there was contact between the spacer spring and the fuel rod. Fretting occurred only where there was a visible gap between the fuel rod and the spring.

Spacer spring relaxation and rod creepdown characteristics have been monitored in relation to burnup on both BWR and PWR fuel rods by measuring the force required to pull a fuel rod through a spacer. Data have been obtained on fuel rods of several reactor types, including ENC 15x15 rods for Westinghouse reactors, which have attained an assembly burnup of 47700 MWd/MTU. Inspection of the 15x15 rods showed no evidence of significant fretting or wear damage at the contact points.

The spacer spring relaxation, based on this and other data, follow an asymptotic relationship with burnup. For the rod and spacer

spring type incorporated in D.C. Cook 1, the average spring force at 47700 MWd/MTU is approximately 8% of the initial spring force. The spring force at the top and bottom of most grids is at least 24% of the initial spring force. A minimum of 8% is required at the rod ends to counter forces produced by flow-induced vibration, while contact is required in the central grids. The residual spring force is, thus, adequate to prevent fretting wear during extended burnup.

Due to the substantial restraint forces remaining at the ends of the rods, the positive flow vibration test results of ENC designs with fully relaxed springs, and the successful irradiation experience of ENC fuel to high burnup levels, the spacer-rod support system is projected to provide ample restraint to prevent fretting vibration to the projected 41,000 MWd/MTU assembly design burnup.

Table 6.1 FUEL ROD PARAMETERS USED IN DESIGN EVALUATION

CLADDING

Inside Diameter

Outside Diameter

Maximum Ovality

PELLET

Outer Diameter

Fractional Dish Volume

Shoulder Width

Fractional Initial Density

Length

Maximum Resinter Densification

ROD

Active Fuel Length

Fill Gas Pressure

XN-NF-84-25 (NP) Page 75

Table 6.2

D.C. COOK UNIT 1 EXTENDED EXPOSURE STUDY - POWER AND FAST FLUX

HISTORY FOR THE PIN WITH MAXIMUM DISCHARGE EXPOSURE

Time During	Pin	Pin	Pin Fast Flux
Exposure	Exposure	Power	(> 1 MeV)
(Hours)	(TM\bWM)	(kW/ft)	$(10^{13} \text{ncm}^{-2} - \text{sec}^{-1})$
0	0	8.82	8.12
1,526	3,091	8.47	8.03
3,358	6,775	8.38	8.21
5,790	10,408	8.25	8.34
6,289	12,562	8.17	8.41
6,289	12,562	7.68	7.90
7,815	15,469	7.76	8.18
9,647	18,823	7.62	8.25
11,479	22,146	7.59	8.44
12,578	24,132	7.59	8.56
12,578	24,132	7.36	8.31
15,088	28,532	7.50	8.75
17,599	33,079	7.70	9.28
20,109	37,679	7.70	9.59
22,619	42,266	7.64	9.81
23,404	43,700	7.64	9.91

Table 6.3
DUTY CYCLES

Type 1 - Ramp to FQ^T or Fractional Increase of Peak Rod	Frequency
Return to 100% Power After Shutdown	19/Year
Step Load Increase (0-40-100)	2/Year
Type 2 - Ramp to 112% of Nominal Power	
Load Follow (100-60-100)	1/Day
Operator Qualification (100-50-100)	12/Year
Operator Qualification (100-80-100)	1/Week

Table 6.4

CLADDING FATIGUE ANALYSIS SUMMARY

Reactor Cycle	Duty Cycle	Peak Stress Amplitude ksi	Actual Cycles, n	Allowable Cycles, N	Usage Factor, n/N
1 (12-Month)	Type I	19,235	21	5,318	0.0039
	Type II	3,025	429	> 106	< 0.0004
2 (12-Month)	Type I	32,545	21	486	0.0432
	Type II	6,810	429	> 106	< 0.0004
3 (18-Month)	Type I	34,595	32	368	0.0870
	Type II	11,360	644	> 104	< 0.0644

 $\sum n/N = 0.20$

Figures 6.1 through 6.5 (pgs. 77-81) have been deleted.

7.0 REFERENCES

- 1. Generic Fuel Design for 15x15 Reload Assemblies for Westinghouse Plants, XN-75-39.
- 2. Not Used.
- 3. ASME Boiler and Pressure Vessel Code, Section III, 1971 Edition, ASME, New York, NY.
- 4. H. S. Rosenbaum, "The Interaction of Iodine with Zr-2", Electrochemical Technology, Volume 4, Number 3-4 (March-April 1966).
- 5. A. Garlick, <u>Stress Corrosion Cracking of Zirconium Alloys in Iodine Vapour</u>, British Energy Conference, London, July 1971.
- 6. R. A. Lorenz, J. L. Collings, S. R. Manning, Fission Product Release From Simulated LWR Fuel, NUREG/CR-0274, ORNL/NUREG/TM-154, October 1978.
- 7. M. Peels, H. Stehle, and E. Steinberg, <u>Out-of-Pile Testing of Iodine Stress Corrosion Cracking in Zircaloy Tubing in Relation to the PCI-Phenomenon</u>, Fourth International Conference on Zirconium in the Nuclear Industry, 1978.
- 8. Nukleare Sicherheit, <u>Halbjahresbericht 1977/1</u>, KFK 2500, Kernforschungszentrum, Karlsruhe, December 1977.
- 9. A. K. Miller, et al, Zircaloy Cladding Deformation and Fracture Analysis EPRI NP-856, August 1978.
- 10. Stress Corrosion Cracking of Zircaloys, SRI International, EPRI NP-1329, March 1980.
- 11. EPRI-NASA Cooperative Project on Stress Corrosion Cracking of Zircaloy, SRI International, EPRI NP-717, March 1978.
- 12. K. R. Merckx, RODEX2 Fuel Rod Thermal-Mechanical Response Evaluation Model, XN-NF-8I-58(P), August 1981.
- 13. RAMPEX Pellet-Clad Interaction Evaluation Code for Power Ramps, XN-NF-573, May 1982.
- 14. A. A. Bauer, L. M. Lowry, and J. S. Perrin, <u>Process on Evaluating Strength and Ductility of Irradiated Zircaloy During July through September 1975</u>. BMI-1938, September 1975.
- A. A. Bauer, L. M. Lowry, W. J. Gallaugher, and A. J. Markworth, Evaluating Strength and Ductility of Irradiated Zircaloy Quarterly Progress Report January through March 1978, NUREG/CR-0085, 8MI-2000, June 1978.

REFERENCES (Continued)

- 16. W. J. O'Donnel and B. F. Langer, "Fatigue Design Bases for Zircaloy Components," Nuclear Science and Engineering, Volume 20, January 1964.
- 17. D. O. Pickman, "Design of Fuel Elements". Unpublished paper prepared for presentation at the "Advanced Course on limiting Aspects of Fuel Element Performance in Water-Cooled Reactors", organized by the Netherlands-Norwegian reactor School at Institutt for Atomenergi, Norway, August 24-28, 1970.
- 18. G. D. Fearnehaugh and A. Cowan, "The Effect of Hydrogen and Strain Rate on the Ductile-Brittle Behavior of Zircaloy", Journal of Nuclear Materials. May 1967, Volume 22, pp. 137-147.
- 19. R. L. Knecht and P. J. Pankaskie, Zircaloy-2 Pressure Tubing, BNWL-746, December 1968.
- 20. H. W. Wilson, K. K. Yoon, and D. L. Baty, "The Effect of Fuel Rod Design on SCC Susceptibility", ANS Light Water Reactor Fuel Performance Conferences, Portland, OR, April 29-May 3, 1979.
- 21. A. A. Bauer, L. M. Lowry, W. J. Gallaugher, and A. J. Markworth, Evaluating Strength and Ductility of Irradiated Zircaloy Quarterly Progress Report July through September 1977, BMI-NUREG-1985, October 1977.
- 22. XN-NF-82-06, Qualification of Exxon Nuclear Fuel for Extended Burnup, June 1982.
- 23. XN-NF-81-58(A), Revision 2, "Fuel Rod Thermal-Mechanical Response Evaluation Model", March 1984.
- 24. XN-NF-75-48, "Definition and Justification of Exxon Nuclear Company DNB Correlation for PWR's", October 1975.
- 25. Not Used.
- 26. XN-NF-75-21(P), Rev. 2, "XCOBRA-IIIC: A Computer Code to Determine the Distribution of Coolant During Steady-State and Transient Core Operation", September 1982.
- 27. Not Used.
- 28. K. P. Galbraith, GAPEX, XN-73-25, August 1973.
- 29. E. Duncombe, Westinghouse (USA) Report, WAPD-TM-794, (1968).

REFERENCES (Continued)

- 30. H. R. Higgy and F. H. Hammad, "Effect of Neutron Irradiation on the Tensile Properties of Zircaloy-2 and Zircaloy-4," J. of Nuclear Materials, 44, August 1972.
- 31. B. Watkins and D. S. Wood, The Significance of Irradiation Induced Creep on Reactor Performance of a Zircaloy-2 Pressure Tube, Applications Related Phenomena for Zirconium and Its Alloys, ASIM-SIP-458, American Society for Testing and Materials, 1969, pp. 226-240.
 - 32. D. Lee, C. F. Shih, F. Zaverl, Jr. and M. D. German, <u>Plastic Theories</u> and Structure Analysis of Anisotropic Metals Zircaloys, EPRI NP-500, RP 456-2, May 1977.
- 33. D. G. Hardy, High Temperature Expansion and Rupture Behavior of Zircaloy Tubing, CONF-730304 USAEC/TIC, Water Reactor Safety, March 26-28, 1973, p. 254-273.
- D. A. Powers, R. O. Meyer, <u>Cladding Swelling and Rupture Models for LOCA Analyses</u>, NUREG-0630, 1981.
- 35. E. Duncombe, F. A. Nichols, S. H. Leiden and W. F. Bourgeois, <u>Prediction of the In-Reactor Deformation of Zircaloy Cladding for Oxide Fuel Rods</u>, WAPD-TM-80C(L), December 1969.
- 36. R. V. Hesketh, J. E. Harbottle, N. A. Waterman and R. C. Loff, "Irradiation Growth and Creep in Zircaloy-2," Radiation Damage in Reactor Materials, Volume 1, Proc. of Vienna Synposium, IAEA-SM-120/D-3, 1969.
- 37. E. R. Gilbert, "In-Reactor Creep of Reactor Materials," Reactor Technology, Volume 14, 1971.
- 38. R. C. Daniel, "In-Pile Dimensional Changes of Zircaloy-4 Tubing Having Low Hoop Stresses," <u>Nuclear Technology</u>, Volume 14, May 1972.
- 39. P. J. Pankaskie, <u>Irradiation Effects on the Mechanical Properties of Zirconium and Dilute Zirconium Alloys</u>, BN-SA-618, July 1976.
- 40. R. V. Hesketh, "Non-Linear Growth in Zircaloy-4", <u>Journal of Nuclear Materials</u>, 30, (1969), Pages 219-221.
- 41. D. R. Packard, <u>An Analytical Expression Factor-Reactor Growth of ENC Fuel Rods</u>, XN-NF-80-37, August 1980.
- 42. D. L. Hagrman, G. A. Reymann and R. E. Mason, "MATPRO Version II (Revision 2), A Handbook of Materials Properties for Use in the Analysis of Light Water Reactor Fuel Rod Behavior, NUREG/CR-0497 TREE-1280, Rev. 2, August 1981.

REFERENCES (Continued)

- 43. J. B. Conway and R. M. Fincel, "The Thermal Expansion and Heat Capacity of UO₂ to 2000°C," Trans. Am. Nucl. Soc., 6, June 1963.
- 44. Lyons, et al, "UO₂ Properties Affecting Performance", <u>Nuclear</u> Engineering Design, 21, pp 184-185 (1972).
- 45. J. A. Christensen, et al, "Melting Point of Irradiated UO2", WCAP-6065, February 1965.
- 46. ANSYS Engineering Analysis System Theoretical Manual, P. C. Kohnke, 1977. ANSYS User's Guide, 1979. Swanson Analysis System, Houston, PA.
- 47. "Preliminary Exxon Nuclear Maneuvering and Conditioning Criteria (PREMACCX)", XN-NF-S30943, Rev. 2, July 1983.
- 48. P. Sharifi and E. P. Popov, <u>Refined Finite Element Analysis of Elastic Plastic Thin Shells of Revolution</u>, December 1969, SESM-69-28, AD-703908.
- 49. S. Timoshenko, Strength of Materials, Part 2, D. Van Nostran, New York, NY, Third Edition, 1956.
- 50. XN-75-27, "Exxon Nuclear Neutronic Design Methods for Pressurized Water Reactors", Exxon Nuclear Company, June 1975.
- 51. S. Timoshenko and J. M. Gere, Theory of Elastic Stability, McGraw-Hill, Inc., New York, 1961.
- 52. R. J. Roark, Formulas for Stress and Strain, McGraw-Hill, Inc., 4th Edition 1965, page 107.
- M. P. Paidoussis and F. L. Sharp, "An Experimental Study of the Vibration of Flexible Cylinders Induced by Nominally Axial Flow", Transactions of American Nuclear Society, 11 (1), pages 352-353, (1968).
- 54. M. P. Paidoussis, The Amplitude of Fluid Induced Vibrations of Cylinder in Axial Flow, AECL-2225, March 1965.
- 55. K. R. Merckx, "Cladding Collapse Calculational Procedure", JN-72-23, November 1972.
- 56. XN-NF-72-23, Revision 1, "Cladding-Collapse Calculational Procedure".

MECHANICAL DESIGN REPORT SUPPLEMENT FOR D.C. COOK UNIT 1 EXTENDED BURNUP FUEL ASSEMBLIES

Distribution

JC Chandler

RA Copeland

NL Garner

NRC/JC Chandler (15)

Document Control (5)

